



Published in final edited form as:

Dev Biol. 2024 January ; 505: 122–129. doi:10.1016/j.ydbio.2023.11.003.

Islet architecture in adult mice is actively maintained by Robo2 expression in β cells

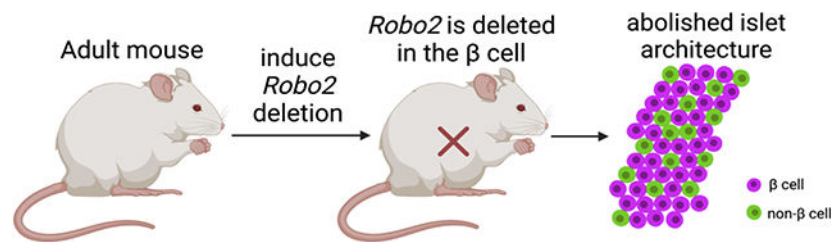
Bayley J. Waters¹, Zoe R. Birman¹, Matthew R. Wagner¹, Julia Lemanski¹, Barak Blum^{1,*}

¹Department of Cell and Regenerative Biology, University of Wisconsin-Madison, Madison, WI 53705, USA

Abstract

A fundamental question in developmental biology is whether tissue architectures formed during development are set for life, or require continuous maintenance signals, and if so, what are those signals. The islets of Langerhans in the pancreas can serve as an elegant model tissue to answer these questions. Islets have a non-random spatial architecture, which is important to proper glucose homeostasis. Islet architecture forms during embryonic development, in a morphogenesis process partially involving expression of Roundabout (Robo) receptors in β cells, and their ligand, Slit, in the surrounding mesenchyme. Whether islet architecture is set during development and remains passive in adulthood, or whether it requires active maintenance throughout life, has not been determined. Here we conditionally deleted *Robo2* in β cells of adult mice and observed their islet architecture following a two-month chase. We show that deleting *Robo2* in adult β cells causes significant loss of islet architecture without affecting β cell identity, maturation, or stress, indicating that Robo2 plays a role in actively maintaining adult islet architecture. Understanding the factors required to maintain islet architecture, and thus optimize islet function, is important for developing future diabetes therapies.

Graphical Abstract



*Corresponding Author: Barak Blum; bblum4@wisc.edu.

Author contributions: BB and BJW conceived and designed experiments. BJW, ZRB, MRW, and JL performed experiments and analyzed data. BB and BJW wrote and edited the manuscript. BB is the guarantor of this work and, as such, had full access to all the data in the study and takes responsibility for the integrity of the data and the accuracy of the data analysis.

Conflict of Interest: The authors declare no conflicts of interests in relation to this work.

Prior Presentation information: This work has been deposited in *bioRxiv* (DOI number [10.1101/2022.09.07.506980](https://doi.org/10.1101/2022.09.07.506980)).

Publisher's Disclaimer: This is a PDF file of an unedited manuscript that has been accepted for publication. As a service to our customers we are providing this early version of the manuscript. The manuscript will undergo copyediting, typesetting, and review of the resulting proof before it is published in its final form. Please note that during the production process errors may be discovered which could affect the content, and all legal disclaimers that apply to the journal pertain.

Introduction

The spatial arrangement of endocrine cell types within the islets of Langerhans is important to regulating blood glucose. β cells in the islet function optimally when in contact with other β cells, whereby they can coordinate insulin secretion (1, 2). Both humans and mice exhibit islet architecture which prioritizes β cell- β cell homotypic interactions (3), with humans showing more complex islet architecture in the form of β cell clusters interspersed with α , δ , and PP cells (4), and mice showing a more uniform β cell core surrounded by a mantle of other endocrine cell types.

Loss of islet architecture is seen in diabetes mellitus in both humans and mice (5–7), but it is unclear whether architecture loss is an attempted adaptation to, or a pathological result of, increased diabetogenic stress. Moreover, evidence suggests that loss of synchronous insulin secretion among β cells contributes to blunted insulin sensitivity over time, potentially exacerbating dysglycemia (8, 9). Thus, understanding factors involved in the formation and maintenance of islet architecture is a key consideration in therapies aimed at improving or replacing native islet function.

Islet architecture is established during development, when endocrine progenitor cells migrate away from the pancreatic ducts and cluster together, simultaneously beginning the differentiation process to achieve their mature endocrine identities (10–12). We previously reported that the axon guidance molecules Roundabout (Robo) receptors are required to establish islet architecture in development (13). Deletion of *Robo2* in the β cells of mice during development results in loss of classic murine core-mantle islet architecture, but does not affect β cell identity, maturation, or stress (Figure 1A). This aberrant islet architecture exhibits significant loss of homotypic β cell- β cell interactions, and reduced synchronicity of β cell insulin pulses (14), with mild perturbations in whole-body glucoregulation under homeostatic conditions (13–15). These data indicate that failure to establish correct islet architecture during development has lifelong consequences on islet function. However, whether normal islet architecture remains in place once established, or requires continued cues to be maintained, has not been determined.

Using temporally-controlled *Robo2* deletion as a model, we assessed whether *Robo2* is involved in continued maintenance of the adult islet. We report that islet architecture is actively maintained in adulthood, and that *Robo2* is required for this maintenance.

Research Design and Methods

Animals:

All animal experiments were approved by the University of Wisconsin-Madison Institutional Animal Care and Use Committee (IACUC) under Protocol #M005221. All mouse strains were maintained on a mixed genetic background. *Ins1-CreERT2* (16), *Robo2^{flx}* (17), and *Rosa26^{lox-stop-lox-H2B-mCherry}* (18) mice were previously described. Control colony mates in all analyses were either Cre+ *Robo2^{+/+}* or Cre+ *Robo2^{flx/flx}* without tamoxifen. Adult mice were enrolled to be at least 10 weeks of age at beginning of tamoxifen dosing. Mice ages in each group are as follows: Cre+ *Robo2^{+/+}* +TAM, N=4, 16 weeks, 23.86 weeks, 27.71

weeks, 27.71 weeks; Cre+ Robo2^{flx/flx} -TAM, N=4, 9.86 weeks, 9.86 weeks, 16 weeks, 19.43 weeks; Cre+ Robo2^{flx/flx} +TAM, N=4, 12.57 weeks, 25.57 weeks, 28.71 weeks, 28.71 weeks.

Tamoxifen solution and dosing:

Tamoxifen solution was prepared as previously described (19). 300mg powdered tamoxifen (Sigma, T5648) was dissolved in 10ml of syringe-filtered corn oil at 50°C for 2 hours, and distributed into 1mL aliquots. Both tamoxifen solution and vehicle solution were stored at 4°C in a light-protected box. TAM and vehicle were preheated at 50°C for 30 minutes before filling syringes each day. Mice were weighed on the first day of dosing, and received 0.12mg/g of this body weight of tamoxifen each day for five days by oral gavage. Mice were sacrificed eight weeks after the last tamoxifen dose for tissue collection.

Tissue collection and sectioning:

Mice were euthanized with CO₂ according to standard protocol and their pancreata immediately collected for fixation. Pancreata were fixed in 4% PFA in PBS for 3 hours at 4°C. Samples were then washed, equilibrated in 30% sucrose in PBS, and embedded in FSC 22 Blue. Tissue was cryosectioned with four 10µm slices per slide, each 400µm apart.

Immunostaining, RNA in situ hybridization, and confocal imaging:

Slides were stained using a standard immunofluorescence protocol. The following primary antibodies were used: guinea pig anti-insulin 1:6 (Agilent, IR002), rabbit anti-glucagon 1:200 (Cell Signaling Technology, 2760S), rabbit anti-somatostatin 1:500 (Phoenix Pharmaceuticals, G-060-03), rabbit anti-Ucn3 1:500 (Phoenix Pharmaceuticals, H-019-29), rabbit anti-MafA 1:200 (Cell Signaling Technology, 79737S), rabbit anti-Pax6 (1:200) (BioLegend, 901301), rabbit anti-Sox9 (1:200) (Novus Biologicals, NBP185551), rabbit anti-Gastrin (1:200) (Cell Marque, 256A-14), goat anti-Pdx1 (1:200) (Abcam, ab47383), and rabbit anti-Aldha1a3 (1:200) (Novus Biologicals, NBP15339). The following secondary antibodies were used: donkey anti-guinea pig AF647 1:500 (Jackson, 706-605-148), donkey anti-rabbit AF488 1:500 (Invitrogen, A21206), and donkey anti-goat AF488 1:500 (Invitrogen, A11055). Cell nuclei were counterstained with DAPI (1:1,000). For Pax6, Sox9, Gastrin, and Pdx1, tissue samples were incubated in 1X Histo VT (0638005) antigen retrieval solution for 20 minutes at 70°C in prior to staining. TUNEL staining was performed following citrate buffer antigen retrieval using an *in situ* cell death detection kit (Roche, 11684795910). Positive control slide was treated with deoxyribonuclease to induce DNA damage (Sigma, D4263).

RNA in situ hybridizations were achieved using the RNAscope Multiplex Fluorescent V2 Assay kit (Cat. No. 323100; Advanced Cell Diagnostics), following the manufacturer protocols (323100-USM and MK 51–150 TN; ACD). Murine probe for Slit2 (#449691) was used. An anti-HRP Cy5.5 secondary antibody (Akoya Bio, NEL766001KT) was diluted 1:500 in TSA Buffer (ACD, 322809) and used to target the RNA probe. Slides were imaged using a Nikon Upright FN1 (UWOIC, grant #1S10OD025040-01) or a Nikon AXR (UWOIC, grant #1S10O34394-01), both provided by the University of Wisconsin Optical Imaging Core, or a Keyence XR8000 microscope.

Analysis and statistics:

Cells were counted from sum intensity projected Z-stack images of islets, comprised of seven 1 μ m slices, using the Cell Counter tool on FIJI as previously described (13). Staining intensities were quantified in QuPath. Groups were compared using a 2-way ANOVA with Bonferroni post-hoc analysis for multiple comparisons. Data are presented as average \pm SEM. All statistics were done using Prism GraphPad. P-values below 0.05 were considered significant.

Data availability:

All data generated during and/or analyzed during the current study are available from the corresponding author on reasonable request.

Results

We aimed to explore a fundamental question in islet development: whether islets of Langerhans, whose tissue architecture is carefully orchestrated during development, require continued maintenance after architecture is established. We have previously shown that expression of Robo in β cells is required for endocrine cell type sorting as mouse islets form during development (13). However, Robo continues to be expressed in the adult islet, and is strongly downregulated in early stages of obesity, concomitant with compensatory islet expansion (13). We hypothesized that Robo is also required for active maintenance of islet architecture in adulthood. To test this hypothesis, we deleted *Robo2* in the β cells of adult mice using an inducible Cre-Lox system. Figure 1B illustrates two possible outcomes following *Robo2* β cell-deletion. If islet architecture does not require active maintenance after being established, then deletion of *Robo2* in adulthood will not impact islet architecture (**top**). If islet architecture does require active maintenance, and Robo2 continues to play a similar role in positional cell guidance in adulthood as it does in development, then intra-islet endocrine cell type admixture is expected following *Robo2* deletion in adults (**bottom**).

To delete *Robo2* in the β cells of mice after they reached adulthood, we used a β cell-specific, estrogen receptor-dependent Cre driver (*Ins1-CreERT2*) to delete the floxed portion of the *Robo2* allele (Supplemental Figure 1A). We administered tamoxifen (TAM) in corn oil via oral gavage (OG) to mice aged 10–29 weeks. Mice received 5 consecutive days of TAM dosing, followed by 8 weeks of rest to allow for reduced Robo2 protein expression and any potential cell movement, before their pancreata were collected for analysis (Figure 1C). Study and control mice also possessed a copy of nuclear fluorescent reporter construct Rosa26^{lox-stop-lox-H2b-mCherry}, which provided an indication of the success of our Cre induction and thus *Robo2* deletion, as β cell nuclei fluoresced mCherry once the associated stop codon was deleted (Supplemental Figure 1A,B).

For quantification of islet architecture, non- β (α and δ) cells were visualized and counted together. For each islet, quantification of the percentage of non- β cells in the islet mantle indicates the relative admixture of islet architecture, with lower percentages indicating more

severe admixture. A standard wildtype mouse islet will have nearly all non- β cells in the islet mantle, approaching a value of 100%.

We found that deletion of *Robo2* in adulthood resulted in a significant reduction in the number of non- β cells in the mantle, indicating a notable loss of normal islet architecture (Figure 1D,E). *Ins1-CreERT2^{Tg/0}; Robo2^{flx/flx}* mice which received TAM (*CreER+ Robo2^{flx/flx} +TAM*) had significantly more intermixed islet architecture than both *Ins1-CreERT2^{Tg/0}; Robo2^{+/+}* mice who received TAM (*CreER+ WT +TAM*, $p=0.0113$), and *Ins1-CreERT2^{Tg/0}; Robo2^{flx/flx}* which did not receive TAM (*CreER+ Robo2^{flx/flx} -TAM*, $p<0.0001$). Thus, our results indicate that *Robo2* is required to maintain islet architecture in adult mice, and more broadly, that islet architecture is not simply “set” during development but requires active maintenance after development is complete.

Disruptions in islet architecture are seen in all forms of diabetes mellitus, including in human patients with diabetes and mouse models of diabetes (5–7). Diabetes also presents with loss of β cell maturity (20), which may contribute to the observed changes in islet architecture. To confirm that architecture changes in our model were not due to loss of β cell maturity, we stained for β cell maturity markers urocortin 3 (*Ucn3*) and *MafA*. We observed no notable differences between the experimental group and *CreER+* wildtype controls in overall expression of *Ucn3* (Figure 2A) and *MafA* (Figure 2B,C), indicating that changes in islet architecture are not due to changes in β cell maturity. Additionally, β cell maturity markers *Pax6* and *Pdx1* were expressed at similar levels between experimental mice and *CreER+* wildtype controls (Figure 2D,E). We also saw no expression of β cell immaturity markers *Sox9* and *Gastrin* in either adult group, in comparison to embryonic day 18.5 controls (Figure 3A,B). Minimal co-expression of β cell disallowed gene *Aldh1a3* was observed in both wildtype and *Robo2* β KO at similar incidence (Figure 3C,D), in comparison to diseased β cells in islets from diabetic *Lep^{ob/ob}* mutant mice (WT vs. *Robo2* β KO, $p=0.99$, WT & *Robo2* β KO vs. *Lep^{ob/ob}*, $p<0.0001$). We also did not see any polyhormonal cells in our analysis. Thus, dedifferentiation of β cells does not explain the alterations seen in islet architecture in the *Robo2* β KO mice.

Similarly, the observed changes in adult islet architecture could not be explained by differences in cell death, as number of TUNEL-positive cells were negligible, and not different among groups (Figure 4A). Presence of *Ins1-CreERT2*-driven mCherry only in β cell nuclei, and not in α or δ cell nuclei, indicates that changes in architecture are not due to β cell transdifferentiation into other endocrine cell types (Figure 4B). Thus, aberrations in islet architecture observed following *Robo2* deletion in adulthood appear to result directly from loss of *Robo2*, and not from β cell dedifferentiation, transdifferentiation, or death, as have been reported in development (13). Ratios of α : β differed significantly among groups, with the *CreER+ Robo2^{flx/flx} -TAM* group having the fewest α : β cells, *CreER+ Robo2^{flx/flx} +TAM* group having more, but the *CreER+ WT +TAM* having the most (Supplemental Figure 1C). These ratio differences may be attributable to the presence of loxP sites, the exposure to tamoxifen, or both. Notwithstanding, *CreER+ WT +TAM* had the highest number of α cells to β cells, suggesting that the abnormal architecture seen in the experimental *CreER+ Robo2^{flx/flx} +TAM* group is not explainable by the presence of relatively more alpha cells. Expression of *Robo* ligand *Slit2* RNA was not visibly different

between *CreER+* *Robo2^{flx/flx}* +TAM and *CreER+* WT +TAM controls (Supplemental Figure 1E); however, further exploration into Slit ligand activity in islet architecture maintenance in the adult mouse will be an important future direction.

Cell type arrangement and cell-cell communication within the islet depend in part on the presence and distribution of adhesion molecules. To this effect, we observed E-cadherin and Cadm1 expression in the islets of our experimental group and their *CreER+* *Robo2* wildtype counterparts. Gross distribution and morphology of adhesion molecules E-cadherin appeared similar between groups (Figure 5A). Cadm1, reported to be an α cell adhesion molecule in the islet (21, 22), is distributed mostly around the periphery of the islet in the *CreER+* *Robo2* wildtype mice, while the *CreER+* *Robo2* β KO mice showed variable distribution of Cadm1 throughout the islet (Figure 5B). We hypothesized that the altered distribution of Cadm1 mirrored the altered distribution of α cells; while indeed this was observed to be mostly true (Supplemental Figure 1D), we saw some Cadm1 expression in cells that were not β , α or δ cells. Detailed analyses and further exploration into the behavior of adhesion molecules such as E-cadherin and Cadm1 in *Robo2* mutant mice will be important to reveal the nature of the architecture defect caused by loss of *Robo2*.

Discussion

We tested the hypothesis that adult islet architecture requires active maintenance, by using an inducible model of *Robo2* β cell deletion. We show that islet architecture requires active signaling maintenance after development is complete. This finding is notable, as it has not been shown to date that islets require continued maintenance cues after they achieve mature architecture. Additionally, our discovery that *Robo2* is necessary to maintain islet architecture in adulthood indicates the potency of *Robo2* as a guidance molecule in the mature islet, since reduction in this receptor alone caused significant cell intermixing and loss of mantle-core architecture despite the presumed presence of all other regulatory cues in the islet.

Our results here show that loss of islet architecture is not due to dedifferentiation of β cells, as β cell maturity marker expression in the *Robo2* β KO mice remains similar to their wildtype counterparts. We also saw no evidence that β cells begin to show expression of immaturity markers or disallowed genes. While E-cadherin expression appears similar between groups, α cell adhesion molecule Cadm1 may be differentially distributed in the *Robo2* β KO islets compared to wildtypes, in line with the admixture of α cells into the β cell core in these islets. In developmental models of *Robo2* β -deletion, where *Robo2* is deleted as the islet forms during development, we see evidence of hyperglucagonemia that may be attributable to loss of optimal cell-cell connections among α cells (15). Similarly, loss of Cadm1 from the islet results in hypersecretion of glucagon (21). It will be important to explore how changes in adhesion among α cells in the *Robo2* β KO mouse may relate to the aberrant islet architecture and elevated glucagon secretion seen in these mice.

This work reveals that not only does *Robo* play a role in the adult islet, but also controls islet architecture under homeostatic conditions, wherein there is no demand on the islet to expand and proliferate. *Robo* is required in endocrine progenitors and embryonic β cells

to establish islet architecture as the islet forms throughout development (13), yet the islet continues to expand after β cells reach maturity. Similarly, islets must expand in response to enhanced demand for insulin, such as in pregnancy or under obesogenic stimulus (23, 24). In all cases where islets expand, whether in development or under certain metabolic conditions, islet architecture must remain consistent to preserve optimal islet function. Indeed, it is hypothesized that the disrupted islet architecture in diabetes represents a collapse of normal architecture as islets fail to remodel under expansion-inducing conditions. Alternatively, loss of islet architecture in diabetes may represent an attempt by islets to “loosen” their structure in order to make remodeling easier in the face of increased insulin demand. In either case, it appears that islets must receive cues to regulate their architecture during proliferation events. It would be interesting to study the role that Robo may play in regulating islet architecture during islet expansion.

Increasingly relevant is the importance of islet architecture in preserving the islet function of donor islets, or in building functional islets from stem cells. Islets in culture are observed to lose their architecture and regain it when transplanted (25). Similarly, islets derived from stem cells function better when induced to form mature architecture (26). Research continues to explore the essential role of extracellular matrix (ECM) proteins in regulating islet architecture, including supplementing Matrigel with key ECM factors (27, 28). Slit is the canonical ligand for Robo receptors, and has also been shown to impact islet formation in developing mice (29). Slit from the pancreatic mesenchyme during development may thus interact with Robo on the developing β cell to direct endocrine cell type sorting (30). It is possible that Slit from peri-islet sources may also interact with Robo on the adult β cell to maintain endocrine cell arrangement in adulthood. Further elucidation of the mechanisms behind Robo’s role in maintaining adult islet architecture, and the source of the ligands by which its function is regulated, may play a key part in maintaining healthy islet architecture in islets intended for transplant.

Supplementary Material

Refer to Web version on PubMed Central for supplementary material.

Acknowledgements:

We would like to thank members of the Blum lab, particularly Dr. Melissa Adams, Dex Nimkulrat, and Cyrus Sethna for fruitful discussion, technical advice, and manuscript edits, and to Debayan De Bakshi for manuscript edits and support. We thank the University of Wisconsin Optical Imaging Core managing director Lance Rodenkirch for microscopy support. Parts of some figures were created with biorender.com.

Funding:

NIH R01DK121706, T32 HD041921, University of Wisconsin-Madison Optical Imaging Core (UWOIC) support grant 1S10OD025040-01.

References

1. Farnsworth NL, Hemmati A, Pozzoli M, and Benninger RK (2014) Fluorescence recovery after photobleaching reveals regulation and distribution of connexin36 gap junction coupling within mouse islets of Langerhans. *The Journal of physiology* 592, 4431–4446 [PubMed: 25172942]

2. Brereton HC, Carvell MJ, Asare-Anane H, Roberts G, Christie MR, Persaud SJ, and Jones PM (2006) Homotypic cell contact enhances insulin but not glucagon secretion. *Biochemical and biophysical research communications* 344, 995–1000 [PubMed: 16643853]
3. Hoang DT, Matsunari H, Nagaya M, Nagashima H, Millis JM, Witkowski P, Periwal V, Hara M, and Jo J (2014) A conserved rule for pancreatic islet organization. *PloS one* 9, e110384 [PubMed: 25350558]
4. Bonner-Weir S, Sullivan BA, and Weir GC (2015) Human Islet Morphology Revisited: Human and Rodent Islets Are Not So Different After All. *The journal of histochemistry and cytochemistry : official journal of the Histochemistry Society* 63, 604–612 [PubMed: 25604813]
5. Brereton MF, Vergari E, Zhang Q, and Clark A (2015) Alpha-, Delta- and PP-cells: Are They the Architectural Cornerstones of Islet Structure and Co-ordination? *The journal of histochemistry and cytochemistry : official journal of the Histochemistry Society* 63, 575–591 [PubMed: 26216135]
6. Steiner DJ, Kim A, Miller K, and Hara M (2010) Pancreatic islet plasticity: interspecies comparison of islet architecture and composition. *Islets* 2, 135–145 [PubMed: 20657742]
7. Adams MT, and Blum B (2022) Determinants and dynamics of pancreatic islet architecture. *Islets* 14, 82–100 [PubMed: 35258417]
8. Matveyenko AV, Liuwantara D, Gurlo T, Kirakossian D, Dalla Man C, Cobelli C, White MF, Copps KD, Volpi E, Fujita S, and Butler PC (2012) Pulsatile portal vein insulin delivery enhances hepatic insulin action and signaling. *Diabetes* 61, 2269–2279 [PubMed: 22688333]
9. Satin LS, Butler PC, Ha J, and Sherman AS (2015) Pulsatile insulin secretion, impaired glucose tolerance and type 2 diabetes. *Mol Aspects Med* 42, 61–77 [PubMed: 25637831]
10. Pan FC, and Wright C (2011) Pancreas organogenesis: from bud to plexus to gland. *Developmental dynamics : an official publication of the American Association of Anatomists* 240, 530–565 [PubMed: 21337462]
11. Shih HP, Wang A, and Sander M (2013) Pancreas organogenesis: from lineage determination to morphogenesis. *Annual review of cell and developmental biology* 29, 81–105
12. Sznurkowska MK, Hannezo E, Azzarelli R, Chatzeli L, Ikeda T, Yoshida S, Philpott A, and Simons BD (2020) Tracing the cellular basis of islet specification in mouse pancreas. *Nature communications* 11, 5037
13. Adams MT, Gilbert JM, Hinojosa Paiz J, Bowman FM, and Blum B (2018) Endocrine cell type sorting and mature architecture in the islets of Langerhans require expression of Roundabout receptors in beta cells. *Scientific reports* 8, 10876 [PubMed: 30022126]
14. Adams MT, Dwulet JM, Briggs JK, Reissaus CA, Jin E, Szulczewski JM, Lyman MR, Sdao SM, Kravets V, Nimkulrat SD, Ponik SM, Merrins MJ, Mirmira RG, Linnemann AK, Benninger RK, and Blum B (2021) Reduced synchronicity of intra-islet Ca(2+) oscillations in vivo in Robo-deficient beta cells. *eLife* 10
15. Adams MT, Waters BJ, Nimkulrat SD, and Blum B (2023) Disrupted glucose homeostasis and glucagon and insulin secretion defects in Robo betaKO mice. *FASEB journal : official publication of the Federation of American Societies for Experimental Biology* 37, e23106 [PubMed: 37498234]
16. Tamarina NA, Roe MW, and Philipson L (2014) Characterization of mice expressing Ins1 gene promoter driven CreERT recombinase for conditional gene deletion in pancreatic beta-cells. *Islets* 6, e27685 [PubMed: 25483876]
17. Lu W, van Eerde AM, Fan X, Quintero-Rivera F, Kulkarni S, Ferguson H, Kim HG, Fan Y, Xi Q, Li QG, Sanlaville D, Andrews W, Sundaresan V, Bi W, Yan J, Giltay JC, Wijmenga C, de Jong TP, Feather SA, Woolf AS, Rao Y, Lupski JR, Eccles MR, Quade BJ, Gusella JF, Morton CC, and Maas RL (2007) Disruption of ROBO2 is associated with urinary tract anomalies and confers risk of vesicoureteral reflux. *Am J Hum Genet* 80, 616–632 [PubMed: 17357069]
18. Blum B, Roose AN, Barrandon O, Maehr R, Arvanites AC, Davidow LS, Davis JC, Peterson QP, Rubin LL, and Melton DA (2014) Reversal of beta cell dedifferentiation by a small molecule inhibitor of the TGFbeta pathway. *eLife* 3, e02809 [PubMed: 25233132]
19. Donocoff RS, Teteloshvili N, Chung H, Shoulson R, and Creusot RJ (2020) Optimization of tamoxifen-induced Cre activity and its effect on immune cell populations. *Scientific reports* 10, 15244 [PubMed: 32943672]

20. Nimkulrat SD, Bernstein MN, Ni Z, Brown J, Kendziorski C, and Blum B (2021) The Anna Karenina Model of beta-Cell Maturation in Development and Their Dedifferentiation in Type 1 and Type 2 Diabetes. *Diabetes* 70, 2058–2066 [PubMed: 34417264]
21. Ito A, Ichiyangi N, Ikeda Y, Hagiyaama M, Inoue T, Kimura KB, Sakurai MA, Hamaguchi K, and Murakami Y (2012) Adhesion molecule CADMI contributes to gap junctional communication among pancreatic islet alpha-cells and prevents their excessive secretion of glucagon. *Islets* 4, 49–55 [PubMed: 22513384]
22. Koma Y, Furuno T, Hagiyaama M, Hamaguchi K, Nakanishi M, Masuda M, Hirota S, Yokozaki H, and Ito A (2008) Cell adhesion molecule 1 is a novel pancreatic-islet cell adhesion molecule that mediates nerve-islet cell interactions. *Gastroenterology* 134, 1544–1554 [PubMed: 18471525]
23. Weir GC, and Bonner-Weir S (2004) Five stages of evolving beta-cell dysfunction during progression to diabetes. *Diabetes* 53 Suppl 3, S16–21 [PubMed: 15561905]
24. Rieck S, and Kaestner KH (2010) Expansion of beta-cell mass in response to pregnancy. *Trends in endocrinology and metabolism: TEM* 21, 151–158 [PubMed: 20015659]
25. Lavallard V, Armanet M, Parnaud G, Meyer J, Barbieux C, Montanari E, Meier R, Morel P, Berney T, and Bosco D (2016) Cell rearrangement in transplanted human islets. *FASEB journal : official publication of the Federation of American Societies for Experimental Biology* 30, 748–760 [PubMed: 26534832]
26. Balboa D, Barsby T, Lithovius V, Saarimaki-Vire J, Omar-Hmeadi M, Dyachok O, Montaser H, Lund PE, Yang M, Ibrahim H, Naatanen A, Chandra V, Vihinen H, Jokitalo E, Kvist J, Ustinov J, Nieminen AI, Kuuluvainen E, Hietakangas V, Katajisto P, Lau J, Carlsson PO, Barg S, Tengholm A, and Otonkoski T (2022) Functional, metabolic and transcriptional maturation of human pancreatic islets derived from stem cells. *Nature biotechnology* 40, 1042–1055
27. Tremmel DM, Sackett SD, Feeney AK, Mitchell SA, Schaid MD, Polyak E, Chlebeck PJ, Gupta S, Kimple ME, Fernandez LA, and Odorico JS (2022) A human pancreatic ECM hydrogel optimized for 3-D modeling of the islet microenvironment. *Scientific reports* 12, 7188 [PubMed: 35504932]
28. Tixi W, Maldonado M, Chang YT, Chiu A, Yeung W, Parveen N, Nelson MS, Hart R, Wang S, Hsu WJ, Fueger P, Kopp JL, Huising MO, Dhawan S, and Shih HP (2023) Coordination between ECM and cell-cell adhesion regulates the development of islet aggregation, architecture, and functional maturation. *eLife* 12
29. Gilbert JM, Adams MT, Sharon N, Jayaraaman H, and Blum B (2021) Morphogenesis of the Islets of Langerhans Is Guided by Extraendocrine Slit2 and Slit3 Signals. *Mol Cell Biol* 41, e0045120 [PubMed: 33318057]
30. Waters BJ, and Blum B (2022) Islet architecture in adult mice is actively maintained by Robo2 expression in β cells. *bioRxiv*, 2022.2009.2007.506980

Highlights

- Whether adult islet tissue architecture requires active maintenance is unknown
- Conditional deletion of Robo2 in adult beta cells leads loss of islet architecture
- Robo-deleted islets do not show loss of beta cell identity, maturation, or stress
- These data show Robo2 plays a role in actively maintaining adult islet architecture
- Reduction of Robo in beta cells during islet expansion may enable islet remodeling

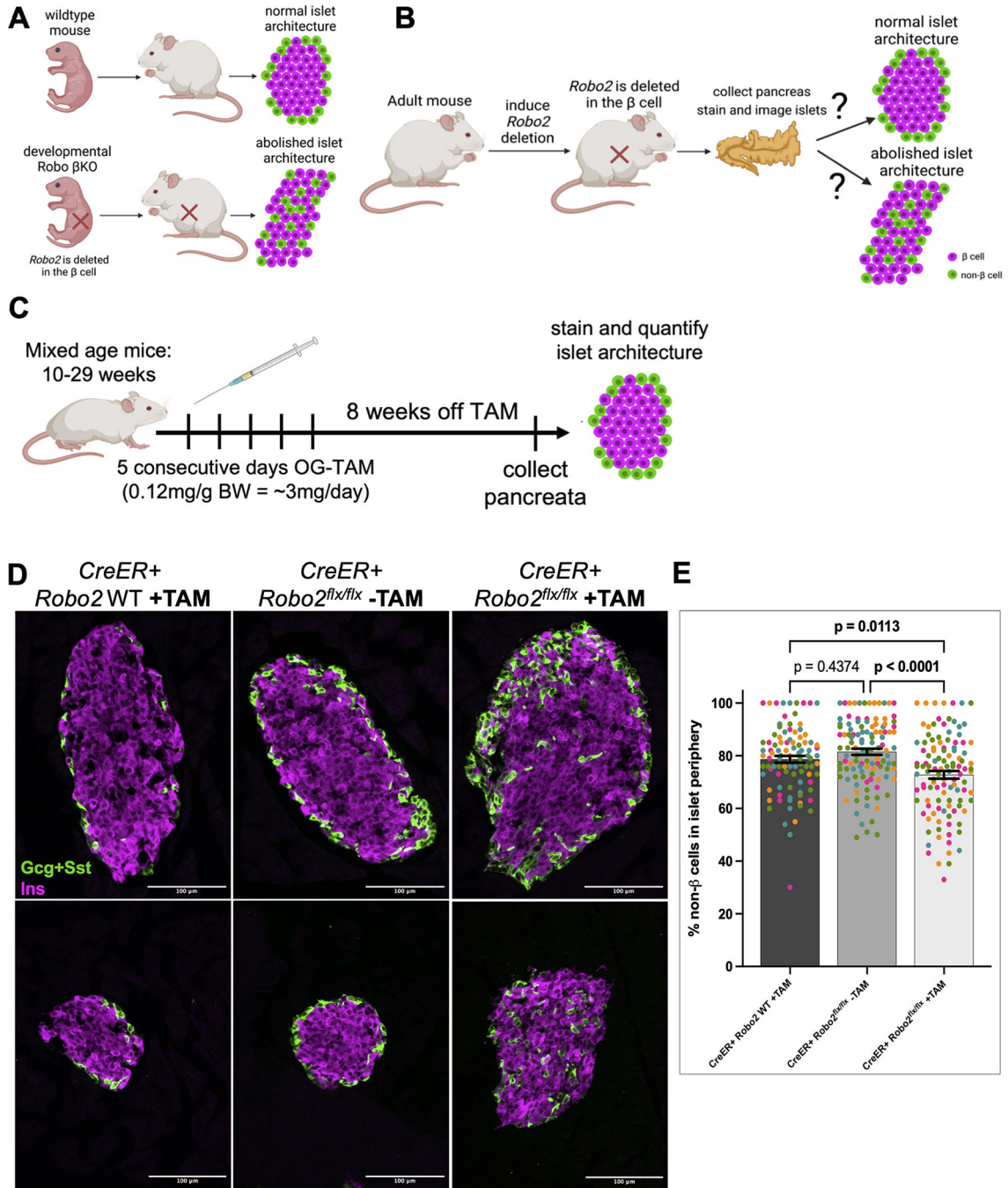


Figure 1: Deleting Robo2 in adult mouse β cells causes significant loss of islet architecture.

(A) Deletion of *Robo2* in the β cells during development results in total loss of islet architecture. (B) Possible outcomes following *Robo2* deletion from the β cells of adult mice. If islet architecture is passive in the adult and does not require maintenance by *Robo2*, the islet will have normal architecture following *Robo2* deletion (top). If *Robo2* is required to actively maintain islet architecture, the islet will exhibit cell type intermixing (bottom). (C) Mice were enrolled to receive tamoxifen (TAM) or vehicle (corn oil) for 5 consecutive days at a dose of 0.12mg/g body weight. 8 weeks following the final dose, mice

were sacrificed and pancreata collected for analysis of islet architecture. **(D)** Representative images of islet architecture in *Robo2*^{+/+} (left), *Robo2*^{flx/flx} mice without TAM induction (middle), and *Robo2*^{flx/flx} mice with TAM induction (right). Top and bottom rows are two representative images for each group. Insulin in magenta, glucagon and somatostatin in green. **(E)** Quantification of the percentage of mantle-localized non- β (α and δ) cells over the total number of non- β cells in the islet. Each color represents different islets from the same mouse. Adult mice with *Robo2* deleted (right bar) show a significantly lower percentage of mantle-localized non- β cells in comparison to controls, indicating disrupted islet architecture. N=4 mice per group, 17–37 islet per mouse, analyzed via 2-way ANOVA with Bonferroni post-hoc test for multiple comparisons.

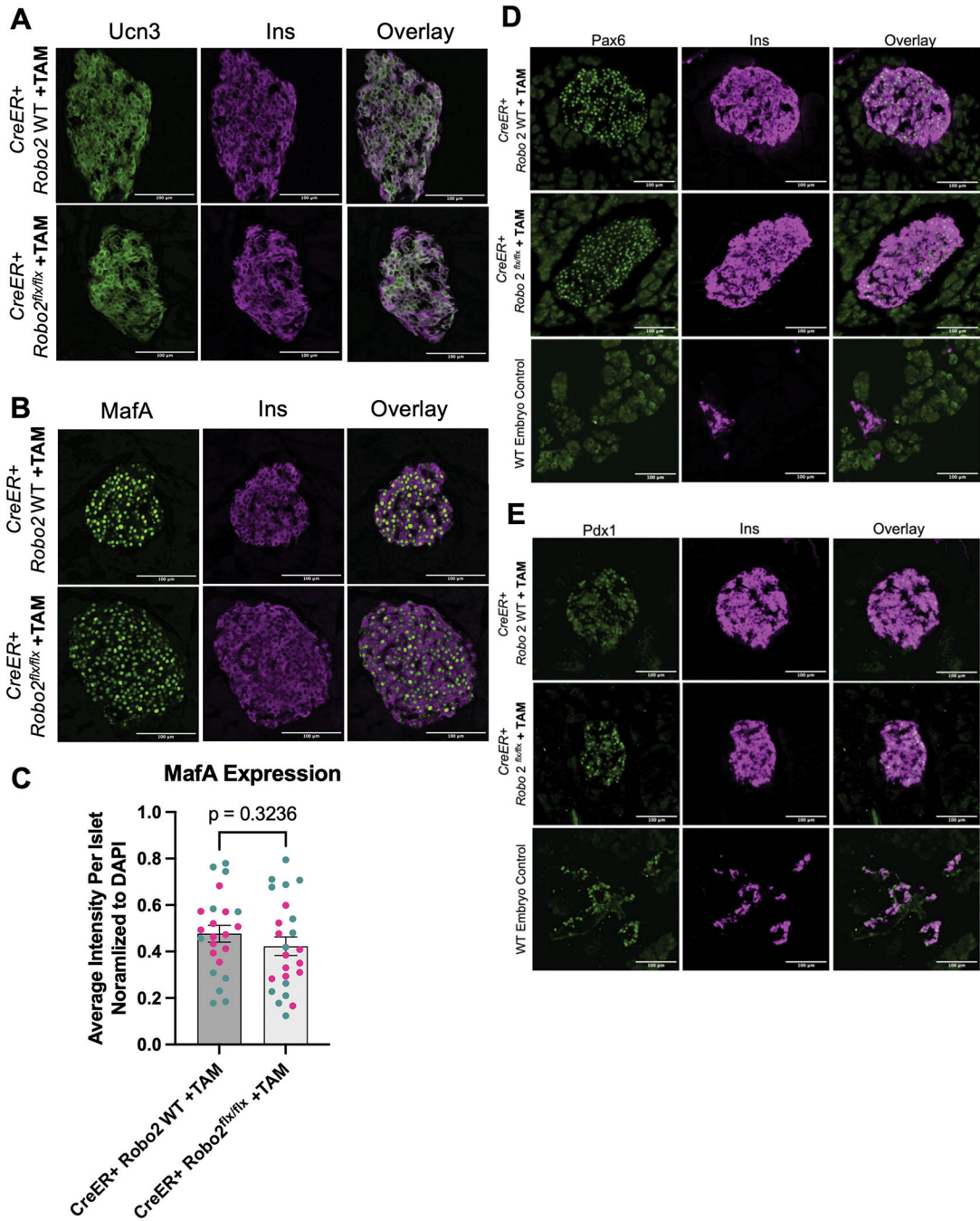


Figure 2: Loss of islet architecture in adult Robo2 mutant mice is not due to loss of β cell maturity.

(A-C) Islets from *Robo2*^{+/+} and TAM-induced *Robo2*^{flx/flx} mice show similar levels of Ucn3 (A) and MafA (B, quantification in C). (D-E) Islets from *Robo2*^{+/+} and TAM-induced *Robo2*^{flx/flx} mice show similar levels of Pax6 (D) and Pdx1 (E) expression.

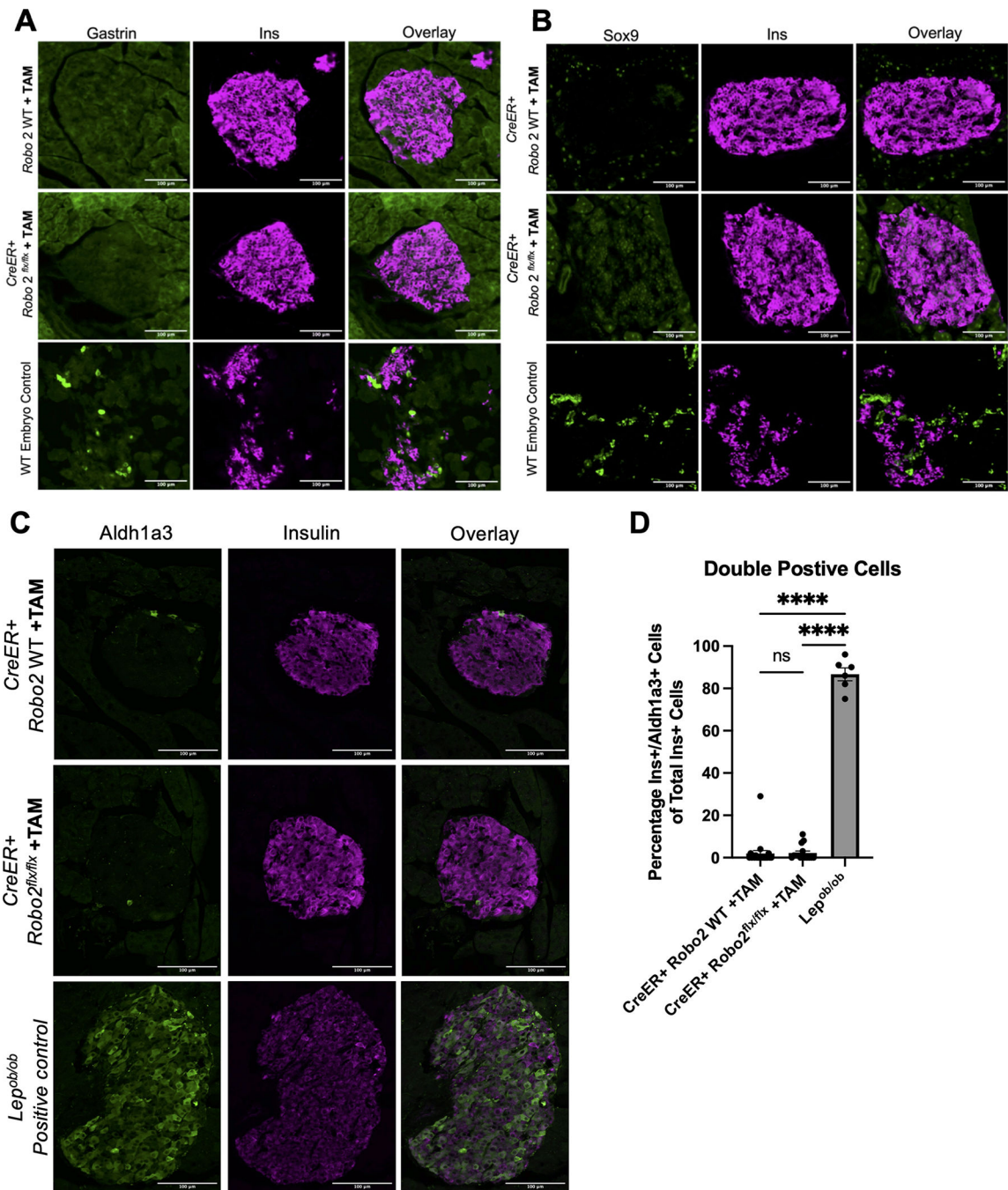


Figure 3: Loss of islet architecture in adult Robo2 mutant mice is not due to β cell dedifferentiation.

(A-B) Islets from Robo^{+/+} and TAM-induced Robo2^{flx/flx} mice do not express β cell immaturity markers Gastrin (A) or Sox9 (B) which are expressed in endocrine progenitors and ductal cells, respectively. (C-D) Islets from Robo^{+/+} and TAM-induced Robo2^{flx/flx} mice show minimal co-expression of β cell disallowed genes in their β cells, and no differences in co-expression.

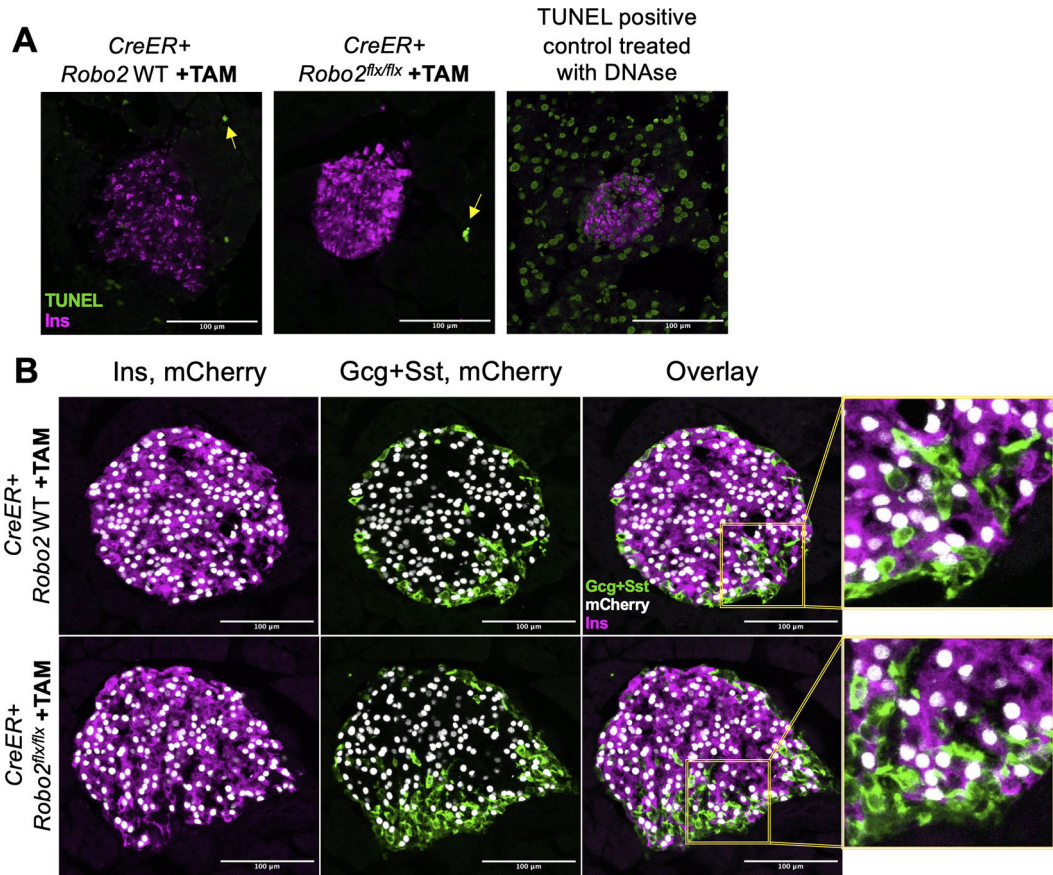


Figure 4: Loss of islet architecture in adult *Robo2* mutant mice is not due to loss of β cell identity or β cell death.

(A) Islets from *Robo2*^{+/+} and TAM-induced *Robo2*^{flx/flx} mice do not have significant differences in cell death (TUNEL). Yellow arrows indicate presence TUNEL staining in cell nuclei. (B) Changes in islet architecture are not due to β cell transdifferentiation, as β cell lineage tracer mCherry localizes only in β cells and not in non- β cells. Insulin in magenta, glucagon and somatostatin in green, mCherry in white.

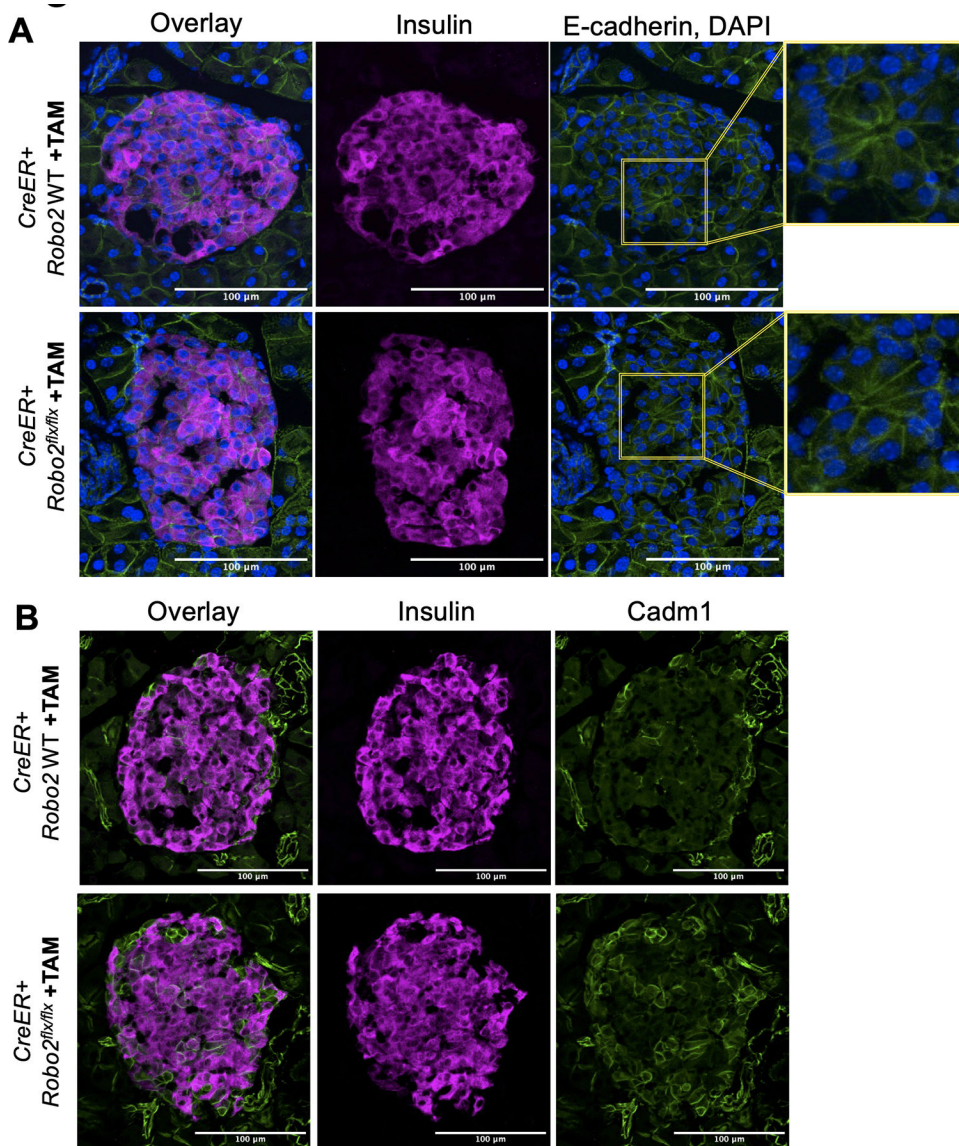


Figure 5: Distribution of adhesion molecules further characterizes adult Robo2 mutant mice. (A-B) Adhesion molecules E-cadherin (A) shows similar distribution across groups. Magnified inserts show examples of β cell rosettes. Distribution of Cadm1 (B) across the islet is altered in the TAM-induced $Robo2^{flx/flx}$ mice, reflecting the intermixing of α cells within the islet. Images were enhanced to aid in visualization of adhesion molecules.